

# The Ultraviolet Luminosity Density of the Universe from Photometric Redshifts of Galaxies in the Hubble Deep Field<sup>1,2</sup>

Sebastian M. Pascarelle and Kenneth M. Lanzetta

Department of Physics and Astronomy, State University of New York at Stony Brook,  
Stony Brook, NY 11794-3800

and

Alberto Fernández-Soto

School of Physics, University of New South Wales, Sydney, NSW2052, Australia

---

<sup>1</sup>Based on observations with the NASA/ESA *Hubble Space Telescope* obtained at the Space Telescope Science Institute, which is operated by AURA, Inc., under NASA Contract NAS 5-26555.

<sup>2</sup>Based in part on observations with the KPNO 4-meter Mayall Telescope of NOAO, which is operated by AURA, Inc., under cooperative agreement with the NSF.

## ABSTRACT

Studies of the Hubble Deep Field (HDF) and other deep surveys have revealed an apparent peak in the ultraviolet (UV) luminosity density, and therefore the star-formation rate density, of the Universe at redshifts  $1 < z < 2$ . We use photometric redshifts of galaxies in the HDF to determine the comoving UV luminosity density and find that, when errors (in particular, sampling error) are properly accounted for, a flat distribution is statistically indistinguishable from a distribution peaked at  $z \simeq 1.5$ . Furthermore, we examine the effects of cosmological surface brightness (SB) dimming on these measurements by applying a uniform SB cut to all galaxy fluxes after correcting them to redshift  $z = 5$ . We find that, comparing all galaxies *at the same intrinsic surface brightness sensitivity*, the UV luminosity density contributed by high intrinsic SB regions increases by almost two orders of magnitude from  $z \simeq 0$  to  $z \simeq 5$ . This suggests that there exists a population of objects with very high star formation rates at high redshifts that apparently do not exist at low redshifts. The peak of star formation, then, likely occurs somewhere beyond  $z > 2$ .

*Subject headings:* galaxies: evolution—galaxies: formation—cosmology: early universe

## 1. Introduction

Important properties of the Universe as a whole can be determined by analyzing complete samples of galaxy redshifts to very faint magnitude limits. The comoving ultraviolet (UV) luminosity density is one such property. Because it is dominated by massive, short-lived stars, the UV emission of an actively star forming galaxy is nearly independent of star formation history. For this reason, the comoving UV luminosity density is directly related to the comoving star formation and metal production rate densities of the Universe (e.g., Cowie 1988; Fall, Charlot, & Pei 1996; Madau *et al.* 1996, hereafter M96). Lilly *et al.* (1996, hereafter L96) measured the UV luminosity density at redshifts  $z \lesssim 1$  using the Canada–France Redshift Survey (CFRS) and found that it rises rapidly by a factor of  $\sim 15$  from  $z = 0$  to  $z = 1$ . Similar results were found in this redshift range by Cowie, Hu, & Songaila (1997).

M96 (later updated by Madau, Pozzetti, & Dickinson 1998, hereafter M98) measured the UV luminosity density at redshifts  $z \simeq 2.75$  and  $z \simeq 4.00$  using the  $U$ - and  $B$ -band “dropout” technique applied to the Hubble Deep Field (HDF) and found that it might be lower than the L96 measurements at  $z \lesssim 1$  by a factor of  $\sim 2$ . This suggested that there might be a peak in the UV luminosity density—and therefore the star formation and metal production rate densities—at some redshift between  $z = 1$  and  $2$ , prompting a spate of theoretical and observational interpretation (e.g., Shaver *et al.* 1996; Baugh *et al.* 1998; Ferguson & Babul 1998; M98; Madau, Della Valle, & Panagia 1998; Silk & Rees 1998). More recently, Connolly *et al.* (1997, hereafter C97) measured the UV luminosity density from the HDF in the previously unsurveyed redshift range  $1 \lesssim z \lesssim 2$  and found that it appears to peak at  $z \simeq 1.5$ , which is consistent with the results of L96 and M98. However the photometric redshifts of galaxies in the HDF from Sawicki, Lin, and Yee (1997) result in a UV luminosity density that continues to increase to  $z \gtrsim 2.5$ , indicating that the peak at  $z \simeq 1.5$  may be questionable.

In this paper, we apply our photometric redshifts of galaxies identified in the HDF (Lanzetta, Yahil, & Fernández-Soto 1996, hereafter LYF96; Lanzetta, Fernández-Soto, & Yahil 1998; Fernández-Soto, Lanzetta, & Yahil 1998, hereafter FLY98) to measure the UV luminosity density of the Universe at redshifts  $0 < z < 6$ . Our analysis differs from previous analyses in three important ways. First, our photometric redshifts are determined from spectral template fits to optimal photometry of optical (Williams *et al.* 1996) and infrared (Dickinson *et al.* 1998) images of the HDF. In contrast to the  $U$ - and  $B$ -band “dropout” technique of M98, our analysis determines the most likely redshift of *every* galaxy in the HDF, and in contrast to the photometric redshifts of C97, our analysis makes use of the  $J$ -,  $H$ -, and  $K$ -band infrared photometry (instead of only the  $J$ -band photometry). Second, we determine realistic uncertainties of the luminosity density measurements, including the effects

of systematic and photometric error on the photometric redshifts and of sampling error. Previous analyses have neglected sampling error, which in fact dominates the uncertainty of the luminosity density measurements in the HDF. Third, we explicitly consider the effects of cosmological  $(1 + z)^3$  surface brightness dimming on the observed luminosity density. Previous analyses have neglected cosmological  $(1 + z)^3$  surface brightness dimming, which varies by more than two orders of magnitude over the redshift range of galaxies identified in the HDF image.

In § 2 we briefly describe our photometric redshift technique. In § 3 we present the results of our measurement of the UV luminosity density, in § 4 we show how this determination is affected by cosmological surface brightness dimming, and in § 5 we discuss these results and present our conclusions.

## 2. Photometric Redshifts

The starting point of our analysis is the photometric redshift estimates of LYF96 and FLY98. Because details of the photometric redshift estimation technique have been and will be presented elsewhere (Lanzetta, Fernández-Soto, & Yahil 1998; FLY98), we simply summarize the method here.

Galaxy photometry is determined from the optical F300W, F450W, F606W, and F814W (Williams *et al.* 1996) and infrared  $J$ ,  $H$ , and  $K$  (Dickinson *et al.* 1998) images of the HDF. To measure fluxes and flux uncertainties in the optical images, we directly integrate within the aperture mask of every object detected in the F814W image. To measure fluxes and flux uncertainties in the infrared images, we (1) model the spatial profile of every object detected in the F814W image as a convolution of the portion of the F814W image containing the object with the appropriate point spread function of the infrared image and (2) determine a least-squares fit of a linear sum of the model spatial profiles to the infrared image. The advantages of this method over simple aperture photometry are that the flux measurements correctly weight signal-to-noise ratio variations within the spatial profiles, and the flux uncertainty measurements correctly include the contributions of nearby, overlapping neighbors.

Galaxy redshifts are determined from fits to the spectral templates of E/S0, Sbc, Scd, and Irr galaxies, including the effects of intrinsic and intervening neutral hydrogen absorption. These effects are included as a function of redshift, with mean values taken from Madau (1995) and Webb (1997). First, we integrate the redshifted spectral templates with the throughputs of the F300W, F450W, F606W, F814W,  $J$ ,  $H$ , and  $K$  filters, at redshifts spanning  $z = 0 - 7$ . Next, we construct the “redshift likelihood function” of every object

detected in the F814W image by calculating the relative likelihood of obtaining the measured fluxes and uncertainties given the modeled fluxes at an assumed redshift, maximizing with respect to galaxy spectral type and arbitrary flux normalization. Finally, we determine the maximum-likelihood redshift estimate of every object detected in the F814W image by maximizing the redshift likelihood function with respect to redshift. The result of the most recent application of this method is presented in the catalog of FLY98, which lists photometric redshift estimates of 1067 galaxies to a limiting magnitude threshold of  $AB(814) = 28.0$  over an angular area of  $\sim 4$  arcmin $^2$ .

Spectroscopic redshifts of more than 100 galaxies in the HDF have been obtained using the Keck telescope (Cohen *et al.* 1996; Cowie 1997; Steidel *et al.* 1996; Zepf *et al.* 1997; Lowenthal *et al.* 1997). Comparison between the spectroscopic and photometric redshifts indicates the following results: (1) At redshifts  $z < 2$ , the residuals between the spectroscopic and photometric redshifts are characterized by an RMS dispersion of  $\sigma = 0.09$  and a discordant fraction ( $> 3\sigma$  discrepant after sigma clipping) of 0%; (2) at redshifts  $z > 2$ , the residuals between the spectroscopic and photometric redshifts are characterized by an RMS dispersion of  $\sigma = 0.45$  and a discordant fraction of 7%; and (3) these residuals between the spectroscopic and photometric redshifts arise from cosmic variance with respect to the spectral templates (rather than from photometric error), so a proper assessment of the errors of the photometric redshifts of faint galaxies must include the effects of systematic and photometric error.

### 3. Ultraviolet Luminosity Density

We determined the luminosity (per unit wavelength interval) of each galaxy at a rest-frame wavelength  $\sim 1500\text{\AA}$  by applying an empirical  $K$ -correction derived from the best-fit spectral template to the measured galaxy photometry. The  $K$ -corrections are *interpolated* from the measured photometry at redshifts  $z > 0.6$ , although they are extrapolated from the measured photometry (by up to a factor of two in wavelength) at redshifts  $z < 0.6$ . Next, we determined the comoving luminosity density versus redshift by arranging the galaxies into redshift bins, summing the luminosities within the bins, and dividing by the appropriate comoving volumes. Finally, we determined the uncertainty of the comoving luminosity density versus redshift by applying a bootstrap resampling technique. For each iteration of the bootstrap technique, we resampled the photometric catalog and redetermined the photometric redshift of each resampled galaxy, perturbing the photometry by random deviates according to the measured photometric error and perturbing the redshift by a random deviate according to the RMS residuals described in §2. We then determined the comoving

luminosity density versus redshift using the resampled, perturbed redshift catalog. We repeated the procedure 1000 times in order to determine the range of values compatible with the observations. This procedure explicitly allows for sampling error, photometric error, and cosmic variance with respect to the spectral templates.

The results are shown in the top panel of Figure 1, which plots the comoving UV luminosity density versus redshift, and are given in the second column of Table 1. For comparison, the data points from L96, C97, and M98 are also plotted in Figure 1a. Note that our data are entirely consistent with the previous measurements to well within  $\simeq 1.5\sigma$  (and all but our first data point are within  $\lesssim 1\sigma$  of previous data). The fact that we do not appear to reproduce the steep rise in the UV luminosity density from  $z = 0 - 1$  of L96 is attributed only to the lowest redshift data point of L96, which is  $\lesssim 1.5\sigma$  discrepant. While this is still consistent with our measurement, the small difference is likely due to the much larger sample of galaxies and the much larger surface area covered by the L96 sample as compared to that of the relatively small HDF field.

Table 1: Comoving UV Luminosity Density

Redshift	Luminosity Density <sup>a</sup>	Luminosity Density above SB Cut	HDF Galaxies	HDF Galaxies above SB Cut
0.00–0.50	$26.29 \pm 0.31$	$24.07 \pm 0.24$	152	1
0.50–1.00	$26.43 \pm 0.23$	$24.98 \pm 0.25$	241	7
1.00–1.50	$26.62 \pm 0.24$	$25.69 \pm 0.11$	228	23
1.50–2.00	$26.65 \pm 0.24$	$25.61 \pm 0.10$	205	49
2.00–3.00	$26.44 \pm 0.28$	$26.24 \pm 0.17$	141	85
3.00–4.00	$26.41 \pm 0.34$	$26.15 \pm 0.15$	62	60
4.00–5.00	$26.52 \pm 0.44$	$26.44 \pm 0.19$	50	50
5.00–6.00	$26.16 \pm 0.59$	$25.77 \pm 0.28$	8	8

<sup>a</sup>Values are log luminosity density at restframe 1500Å in units of  $h_{100}^{-2}$  erg s $^{-1}$  Hz $^{-1}$  Mpc $^{-3}$  ( $q_0=0.5$ ). Errors include the effects of systematic and photometric error on the photometric redshifts and of sampling error.

With sampling errors properly accounted for, the errorbars generated from our bootstrap code are more than a factor of two larger than those of C97 or M98 for the  $z > 2$  UV luminosity density. It can be seen that, after an increase at redshifts  $z \simeq 0 - 2$ , the UV luminosity density remains constant to within errors to redshifts  $z \simeq 6$ . In other words, *we find no convincing evidence that the UV luminosity density decreases with redshift for  $z > 2$ .*

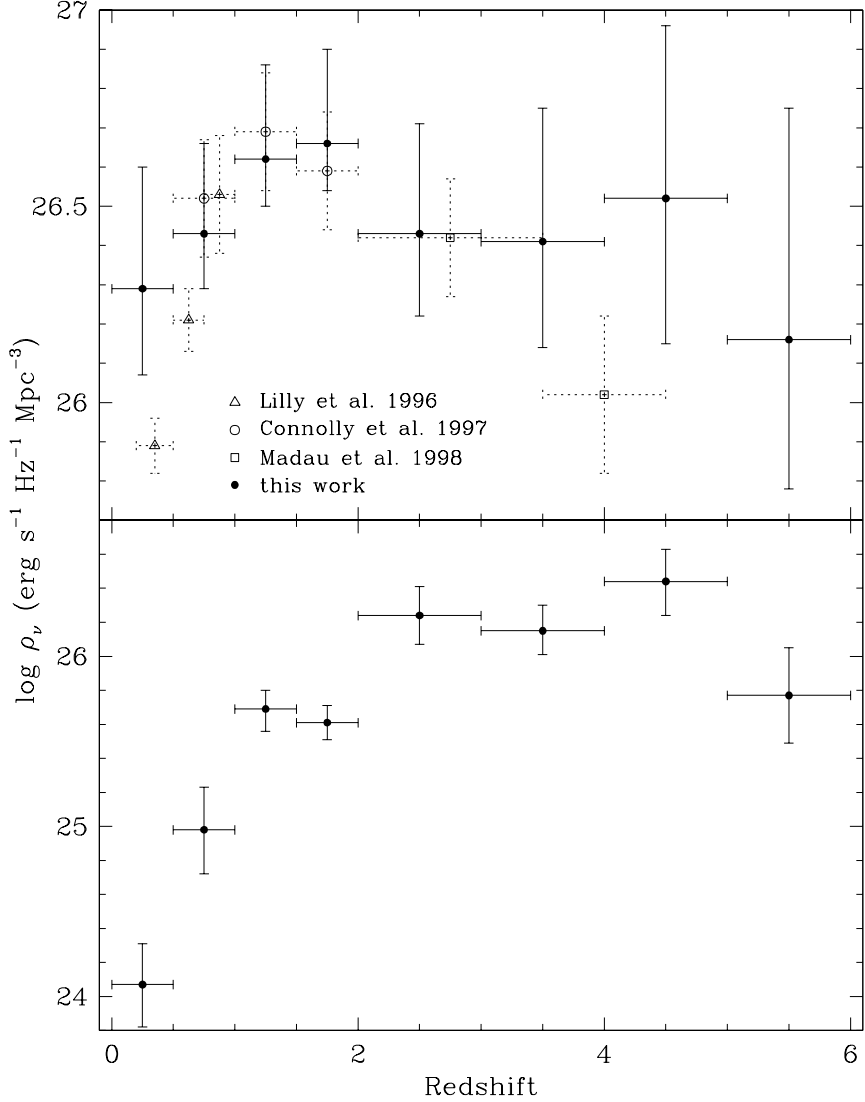


Fig. 1.— (a), The UV luminosity density as a function of redshift as measured from galaxies in the HDF using our photometric redshifts (filled circles). The errorbars were calculated from a bootstrapping code which takes into account the effects of systematic and photometric error on the photometric redshifts and the effects of sampling error. For comparison, we have included data points from Lilly *et al.* (1996, open triangles), Connolly *et al.* (1997, open circles), and Madau *et al.* (1998, open squares). Note that while our data appear to show a possible increase in the UV luminosity density from  $z = 0 - 2$ , there is little evidence for a decrease at higher redshifts to within the errors. (b), The UV luminosity density arising from intrinsically high surface brightness (SB) regions, after applying a uniform SB cut so that  $z < 5$  galaxies are considered down to the same SB level as  $z \gtrsim 5$  galaxies. Comparing the HDF galaxies at the same intrinsic SB sensitivity shows that the UV luminosity density of high SB regions increases by almost two orders of magnitude from  $z \simeq 0$  to  $z \simeq 5$ .

#### 4. Effects of Cosmological $(1 + z)^3$ Surface Brightness Dimming

To meaningfully compare the comoving UV luminosity density of the local, low-redshift Universe with that of the distant, high-redshift Universe, it is necessary to account for the very large effect of cosmological  $(1 + z)^3$  surface brightness (SB) dimming. Because low-redshift galaxies are viewed to much lower *intrinsic* SB thresholds than are high-redshift galaxies, certain corrections must be applied in order to view all galaxies at a common intrinsic SB threshold.

We applied these corrections to our catalog of 1067 galaxies. First, we corrected the flux of each galaxy to the value that would be observed if the galaxy were placed at redshift  $z = 5$ . Specifically, we applied monochromatic SB corrections and  $K$ -corrections on a pixel-by-pixel basis, as in Bouwens, Broadhurst, & Silk (1998), and we also applied small corrections to account for the different *WFPC2* passbands that sample rest-frame 1500 Å at different redshifts.

Next, we applied a uniform SB cut on a pixel-by-pixel basis, excluding pixels that failed to meet a minimum SB threshold. The threshold was determined by assuming that objects are detected in the F814W image to within  $\sim 1\sigma$  of sky, which corresponds to a SB of  $1.27 \times 10^{-33}$  erg s $^{-1}$  cm $^{-2}$  Hz $^{-1}$  pixel $^{-1}$ . Next, we reversed the monochromatic SB corrections and  $K$ -corrections on a pixel-by-pixel basis to bring each galaxy back to its actual redshift and again calculated the comoving luminosity density versus redshift. In this way, only those parts of the galaxies that are of high enough intrinsic SB to be detected at all redshifts up to  $z = 5$  — given the actual sensitivity of the HDF F814W image — are included into the measurement.

Results are shown in the bottom panel of Figure 1, which plots the comoving UV luminosity density versus redshift of high intrinsic surface brightness regions, and in the third column of Table 1. Also listed in Table 1 are the number of galaxies within each redshift bin and the number of galaxies in each bin that have at least one pixel above the SB cut. It is evident that (1) the comoving UV luminosity density of high intrinsic surface brightness regions increases by two orders of magnitude from  $z \simeq 0$  to  $z \simeq 5$ , and (2) star-forming objects seen at  $z > 2.5$  are relatively rare at  $z < 2.5$ . In other words, *the comoving UV luminosity density contributed by high intrinsic SB regions appears to increase monotonically with redshift, at least out to  $z \simeq 5$ .*

## 5. Discussion and Conclusions

Previous determinations of the comoving UV luminosity density at  $z > 2$  rely primarily on the M98 Lyman break galaxy sample. The stated uncertainties of these measurements include contributions from incompleteness at the faint end of the luminosity function (LF) as well as from the volume normalization and color selection region. While these effects do indeed contribute to the total uncertainty, they are by no means the dominant factors. For any LF with power-law index  $\alpha < 2$ , the luminosity density is dominated by the *bright* end of the LF. Because the bright end of the LF is inherently poorly sampled, this sampling error at the bright end of the LF in fact dominates the uncertainty of the luminosity density. Indeed, at redshifts  $z > 2$ , our uncertainties — which include the effects of sampling error — are more than two times larger than those quoted by C97 and M98. This calls into question the statistical significant of the “peak” in the comoving UV luminosity density at  $z \simeq 1.5$ .

Ignoring errors, one can see from Figure 1a that our  $z = 4$  measurement of the UV luminosity density is higher than that of M98. It is possible that this arises because the M98 method of finding galaxies at that redshift *by their definition* does not find all galaxies at  $z \simeq 4$ . Rather, their color-color polygon was designed to find objects that are almost certainly at  $z \simeq 4$  with little contamination from low-redshift objects, which is why the data points of M98 were plotted as lower limits. In Figure 2, we plot the  $z \simeq 4$  objects from our photometric redshift catalog with the M98 polygon. One can see that even with the large  $(B - V)$  errors involved, the M98 technique may be missing half of the high-redshift galaxies in the HDF.

Perhaps the single most important factor that must be included in such a study is the enormous effect of the cosmological surface brightness dimming at very high redshifts. At  $z < 0.1$  this effect is less than a factor of 1.3, but at  $z = 5$  it becomes a factor of 216. Therefore, if we are to compare the UV luminosity density at  $z = 5$  to that of the local Universe, we must consider local galaxies only down to the same SB level as that sampled at high-redshift.

At the highest redshifts, the severe cosmological SB dimming affecting the HDF observations allows only the very highest levels of UV luminosity “column density” (or equivalently, star formation rate “column density”) to be sampled. At progressively lower redshifts, we are able to observe galaxies down to lower and lower SB thresholds. The uniform SB cut that we applied to our galaxy sample to allow for this discrepancy corresponds to a star formation rate column density of  $\simeq 0.1h_{100}^2 M_{\odot} \text{ yr}^{-1} \text{ kpc}^{-2}$  at  $z = 5$  (assuming  $q_0 = 0.5$  and using the relation of UV luminosity to star formation rate with a Salpeter IMF from M98). As seen in Table 1 and the bottom panel of Figure 1, almost no  $z < 1$  objects have star formation rates above this level, while at high redshifts, there are many objects exceeding

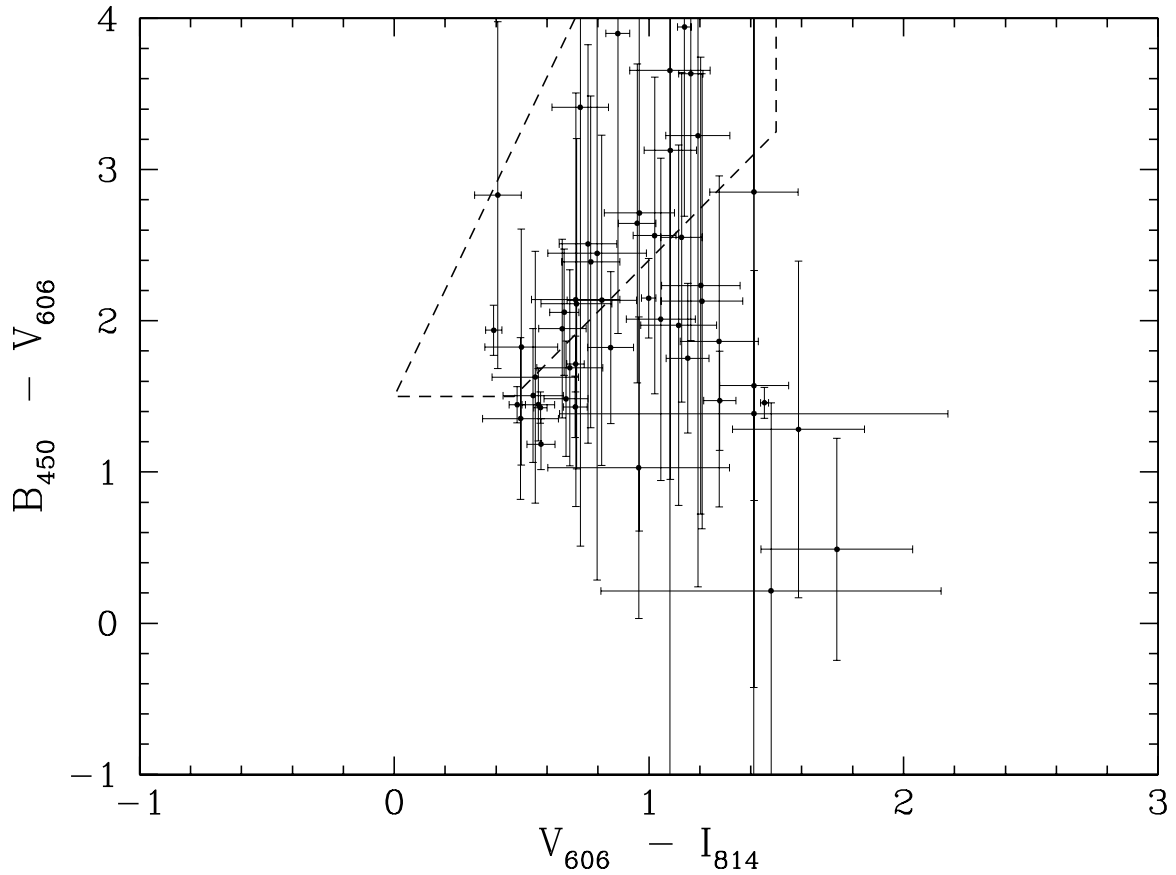


Fig. 2.— Color-color diagram similar to that of Madau *et al.* (1996, 1998) containing  $z \simeq 4$  galaxies selected from our photometric redshift catalog of HDF galaxies and plotted with their measured photometric errors. It can be seen that, while this technique does locate  $z \simeq 4$  galaxies, almost 50% of them may lie outside the selection polygon despite the large ( $B - V$ ) errors involved.

this cut. For example, only 7 out of 241 galaxies from the  $z = 0.5 - 1.0$  redshift bin would be visible at  $z = 5$ , and then only the brightest few image pixels of those objects would peak above the SB cutoff.

Figure 1 provides us with another piece of evidence in favor of a UV luminosity density that increases with redshift. In the lowest redshift bin ( $z = 0.0 - 0.5$ ) of Figure 1a and b, where the SB effect is smallest, the intrinsically high SB regions make up only 0.5% of the total UV luminosity density. If this ratio is the same at high redshifts as it is at low redshifts then our measurements of the UV luminosity density at high redshifts in Figure 1a may need to be increased by up to a factor of 150. Although this ratio may be quite different at high redshifts than it is at low redshifts, this suggests that the UV luminosity density could be a strongly increasing function of redshift.

We have shown that when the low- and high-redshift Universes are observed on equal footing, one gets a completely different impression of the global UV luminosity density than previously thought. We find that objects with star formation rates comparable to those at  $z \gtrsim 3$  are very rare in the nearby Universe. This implies that a majority of the star formation may have occurred at very high redshifts, and therefore that a peak in the star formation rate density of the Universe has not yet been observed and likely lies somewhere at  $z > 2$ .

SMP and KML acknowledge support from NASA grant NAGW-4422 and NSF grant AST-9624216. AF acknowledges support from a grant from the Australian Research Council.

## REFERENCES

Baugh, C. M., Cole, S., Frenk, C. S., & Lacey, C. G. 1998, ApJ, 498, 504  
Bouwens, R., Broadhurst, T., & Silk, J. 1998, ApJ (submitted, preprint astro-ph/9710291)  
Cohen, J. G., Cowie, L. L., Hogg, D. W., Songaila, A., Blandford, R., Hu, E. M., & Shopbell, P. 1996, ApJ, 471, L5  
Connolly, A. J., Szalay, A. S., Dickinson, M., SubbaRao, M. U., & Brunner, R. J. 1997, ApJ, 486, L11  
Cowie, L. L. 1988, in The Post-Recombination Universe, eds Kaiser, N. & Lasenby, A. (Dordrecht, Kluwer) 1  
Cowie, L. L., Hu, E. M., & Songaila, A. 1997, ApJ, 481, L9  
Cowie, L. L. 1997, <http://www.ifa.hawaii.edu/~cowie/tts/tts.html>  
Dickinson, M. *et al.* 1998 (in preparation)

Fall, S. M., Charlot, S., & Pei, Y. 1996, ApJ, 464, L43

Ferguson, H. C., & Babul, A. 1998, MNRAS, 296, 585

Fernández-Soto, A., Lanzetta, K. M., & Yahil, A. 1998, ApJ (in press)

Lanzetta, K. M., Yahil, A., & Fernández-Soto, A. 1996, Nature, 381, 759

Lanzetta, K. M., Fernández-Soto, A., & Yahil, A. 1998, in “The Hubble Deep Field,” proceedings of the Space Telescope Science Institute 1997 May Symposium, ed. M. Livio, S. M. Fall, and P. Madau (in press, preprint astro-ph/9709166)

Lilly, S. J., & Le Fèvre, O., Hammer, F., & Crampton, D. 1996, ApJ, 460, L1

Lowenthal, J. D. *et al.* 1997, ApJ, 481, 673

Madau, P. 1995, ApJ, 441, 18

Madau, P., Ferguson, H. C., Dickinson, M., Giavalisco, M., Steidel, C. C., & Fruchter, A. 1996, MNRAS, 283, 1388

Madau, P., Pozzetti, L., & Dickinson, M. 1998, ApJ, 498, 106

Madau, P., Della Valle, M., & Panagia, N. 1998, MNRAS, 297, 17

Sawicki, M. J., Lin, H., & Yee, H. K. C. 1997, AJ, 113, 1

Shaver, P. A., Wall, J. V., Kellermann, K. I., Jackson, C. A., & Hawkins, M. R. S. 1996, Nature, 384, 439

Silk, J., & Rees, M. J. 1998, A&A, 331, L1

Steidel, C. C., Giavalisco, M., Dickinson, M., & Adelberger, K. L. 1996, AJ, 112, 352

Webb, J. K. 1997, (private communication)

Williams, R. E., *et al.* 1996, AJ, 112, 1335

Zepf, S. E., Moustakas, L. A., & Davis, M. 1997, ApJ, 474, L1